

# On the use of Fourier averages to compute the global isochrons of (quasi)periodic dynamics

A. Mauroy<sup>a)</sup> and I. Mezić<sup>b)</sup>

Department of Mechanical Engineering, University of California Santa Barbara, Santa Barbara, California 93106, USA

(Received 27 March 2012; accepted 25 June 2012; published online 18 July 2012)

The concept of isochrons is crucial for the analysis of asymptotically periodic systems. Roughly, isochrons are sets of points that partition the basin of attraction of a limit cycle according to the asymptotic behavior of the trajectories. The computation of global isochrons (in the whole basin of attraction) is however difficult, and the existing methods are inefficient in high-dimensional spaces. In this context, we present a novel (forward integration) algorithm for computing the global isochrons of high-dimensional dynamics, which is based on the notion of Fourier time averages evaluated along the trajectories. Such Fourier averages in fact produce eigenfunctions of the Koopman semigroup associated with the system, and isochrons are obtained as level sets of those eigenfunctions. The method is supported by theoretical results and validated by several examples of increasing complexity, including the 4-dimensional Hodgkin-Huxley model. In addition, the framework is naturally extended to the study of quasiperiodic systems and motivates the definition of generalized isochrons of the torus. This situation is illustrated in the case of two coupled Van der Pol oscillators. © 2012 American Institute of Physics. [<http://dx.doi.org/10.1063/1.4736859>]

**An efficient way to study asymptotically periodic systems is to consider phase differences between the trajectories, a framework that leads to a powerful dimensional reduction of the system to a one-dimensional model. However, the price to pay for such a reduction is the computation of particular sets of the state space, i.e., the so-called *isochrons*. The computation of isochrons is particularly intricate in high-dimensional spaces—where the isochrons can exhibit a complex geometry—and the existing methods are typically limited to 2-dimensional systems. In contrast, this paper proposes a novel algorithm that is well-suited to the computation of isochrons in high-dimensional spaces. More precisely, we show that the isochrons can be obtained through the computation of Fourier averages evaluated along the trajectories. As a consequence, we obtain a relationship between isochrons and level sets of a class of eigenfunctions of the Koopman semigroup associated with the system. We apply the method to various examples and also extend the framework to quasiperiodic systems.**

## I. INTRODUCTION

According to the seminal works,<sup>8,23</sup> a dynamical system with a stable limit cycle can be reduced to a phase model. In other words, a limit-cycle oscillator (evolving in a high-dimensional space) is equivalent to a phase oscillator (evolving on the one-dimensional circle), a reduced model that is more amenable to mathematical analysis (see Ref. 5 for a review). Phase reduction thereby appears as a useful frame-

work to analyze the sensitivity and the robustness of limit cycles,<sup>20</sup> to compare and design models of oscillators,<sup>14</sup> and to study the collective behaviors of interacting oscillators (see, e.g., the Kuramoto model<sup>17</sup>).

A phase model is obtained by assigning a phase variable to each point in the basin of attraction of the limit cycle. First, the phase is defined on the limit cycle (up to a given reference) as the quantity proportional to the time spent on the cycle. Then, the notion of phase is extended to the whole basin of attraction through the *isochrons* (the term was originally coined in Ref. 24), a concept that corresponds to the invariant fibration of the stable manifold of the limit cycle. In other words, the isochrons partition the basin of attraction in such a way that trajectories starting from the same isochron asymptotically converge to the same orbit on the limit cycle.

The computation of isochrons is desirable not only to obtain a phase reduction of the system but also to provide a global picture of the system dynamics as well as an insight into the sensitivity to external perturbations. Local isochrons—in the vicinity of the limit cycle—are obtained using either linearization techniques (and higher order approximations<sup>18,19</sup>) or standard backward integration methods (see Ref. 6 for a detailed example of the algorithm). In contrast, the computation of global isochrons—in the entire basin of attraction—is much more involved and has only been investigated in a few studies, most of which propose numerical schemes based on the extension of local isochrons through backward integration.<sup>2,16</sup> In addition, the computation of global isochrons is particularly difficult for dynamics with multiple time scales (slow-fast dynamics) and for high-dimensional dynamics, two situations where backward integration is inefficient owing to numerical sensitivity issues. While an elegant method is provided in Ref. 12 to compute the global isochrons

<sup>a)</sup>Electronic mail: alex.mauroy@enr.ucsb.edu.

<sup>b)</sup>Electronic mail: mezcic@enr.ucsb.edu.

of systems with multiple time scales, there is so far no efficient method in the case of high-dimensional dynamics.

In this paper, we present a novel method for computing the global isochrons of high-dimensional dynamics. The method is a forward integration method that relies on the *time-averaging of observables* along the trajectories of the system. Originally, the use of time averages was devoted to the visualization of invariant ergodic partitions.<sup>11</sup> However, the levels sets of “generalized” time averages—the *Fourier averages*—identify subsets of the state space that are mapped to themselves with a given frequency,<sup>9,10</sup> subsets that correspond to isochrons in the case of asymptotically periodic systems. When combined with suitable interpolation techniques, the computation of time averages is a well-developed framework which is not restricted to low-dimensional systems, thereby yielding a convenient and flexible method to obtain global isochrons in high-dimensional spaces.

The proposed method is derived from a general theoretical background—the isochrons being related to the eigenfunctions of the *Koopman semigroup* associated with the system (Ref. 13)—so that it can be applied to systems that are not periodic. For a (normally hyperbolic) attractor that is not a limit cycle, an invariant fibration of the stable manifold always exists,<sup>3,22</sup> but the existence of a phase parametrization (of the attractor and its basin of attraction) is not guaranteed. In the particular case of quasiperiodic systems, phase coordinates are introduced in the whole basin of attraction through the *generalized isochrons*, a new concept that appears as a natural extension of the framework developed in the present paper. The intersections of these generalized isochrons correspond to the invariant fibration of the stable manifold.

The paper is organized as follows. In Sec. II, we present the theoretical results that support our method based on the computation of Fourier averages. Both relevance and validity of the method are emphasized in Sec. III, where the isochrons are computed for several models of increasing complexity, including the (high-dimensional) Hodgkin-Huxley model. In Sec. IV, we consider the case of quasiperiodic dynamics and show that the method can be used to compute the generalized isochrons of the 2-dimensional torus. Finally, the paper closes with some concluding remarks in Sec. V.

## II. ISOCHRONS AND FOURIER AVERAGES

### A. Preliminaries

We consider a dynamical system

$$\dot{x} = F(x) \quad x \in \mathbb{R}^n, \tag{1}$$

which admits a (exponentially) stable limit cycle  $\Gamma$  of period  $T_0$ , with a basin of attraction  $\mathcal{B}(\Gamma) \subseteq \mathbb{R}^n$ . In addition, we let  $\phi : \mathbb{R}^+ \times \mathbb{R}^n \mapsto \mathbb{R}^n$  denote the flow induced by Eq. (1), i.e.,  $\phi(x_0, t)$  is the solution of Eq. (1) with the initial condition  $x_0$ .

According to Ref. 8, a phase  $\theta \in \mathbb{S}^1(0, 2\pi)$  can be assigned to each point of the limit cycle. Namely, a point  $x^\gamma \in \Gamma$  has a phase  $\theta = 2\pi t/T_0$ , where  $t < T_0$  is such that  $\phi(t, x_0^\gamma) = x^\gamma$  ( $x_0^\gamma \in \Gamma$  is an arbitrarily chosen point of the limit cycle that corresponds to phase  $\theta = 0$ ). It follows from

this definition that an orbit on the limit cycle in  $\mathbb{R}^n$  obeys the phase dynamics  $\dot{\theta} = \omega_0$  on  $\mathbb{S}^1$ , with  $\omega_0 = 2\pi/T_0$ .

Next, the above framework is extended to the whole basin of attraction through the introduction of isochrons. An isochron is defined as follows:

*Definition 1.* An isochron—associated with the phase  $\theta \in \mathbb{S}^1$ —of the limit cycle  $\Gamma$  is the  $(n - 1)$ -dimensional manifold  $\mathcal{I}_\theta$  defined as

$$\mathcal{I}_\theta = \{x \in \mathcal{B}(\Gamma) \mid \lim_{t \rightarrow \infty} \|\phi(t, x) - \phi(t + \theta/(2\pi)T_0, x_0^\gamma)\| = 0\}.$$

Roughly speaking, a trajectory with the initial condition  $x \in \mathcal{I}_\theta$  asymptotically approaches a (periodic) trajectory on the limit cycle characterized by an initial condition associated with the phase  $\theta$ . Since the two trajectories have the same asymptotic behavior, whether the initial condition is on the limit cycle or not, the phase  $\theta$  can also be assigned to the initial condition  $x \notin \Gamma$ .

It also follows from Definition 1 that the isochrons correspond to subsets of  $\mathcal{B}(\Gamma)$  that are invariant under the time- $T_0$  map  $\phi(T_0, \cdot)$ .

### B. Fourier averages

In this section, we show the strong connection between the isochrons of the limit cycle and the *Fourier averages* evaluated along the trajectories. The Fourier averages of an *observable*  $f : \mathbb{R}^n \mapsto \mathbb{R}$  (assumed to be continuously differentiable) are given by

$$f_\omega^*(x) = \lim_{T \rightarrow \infty} \frac{1}{T} \int_0^T (f \circ \phi_t)(x) e^{-i\omega t} dt, \tag{2}$$

with the notation  $\phi_t(x) = \phi(t, x)$ . For a fixed  $x$ , Eq. (2) is equivalent to a Fourier transform of the (time-varying) observable computed along a trajectory. Hence, for a dynamics with a stable limit cycle (of frequency  $\omega_0$ ), it is clear that the Fourier average can be nonzero only for the frequencies  $\omega = k\omega_0, k \in \mathbb{Z}$ .

It is remarkable that the isochrons are the level sets of the Fourier averages  $f_{k\omega_0}^*$ . Indeed, the Fourier averages are the eigenfunctions of the Koopman semigroup of operators  $U^t$  defined by  $U^t f(x) = f \circ \phi_t(x)$ : they satisfy  $U^t f_{k\omega_0}^*(x) = \exp(ik\omega_0 t) f_{k\omega_0}^*(x)$  (Refs. 9, 10, and 13) (note that the modulus of the eigenfunctions is constant, thus restricting the values to a circle in the complex plane). Then, each level set of a Fourier average is invariant under the time- $T_0$  map  $\phi(T_0, \cdot)$ , a property that is also satisfied by the isochrons. The exact relation between the Fourier averages and the isochrons is summarized in the following proposition.

*Proposition 1.* Consider an observable  $f \in C^1$  such that the first Fourier coefficient of the  $T_0$ -periodic function  $f^\Gamma(t) \triangleq (f \circ \phi_t)(x_0^\gamma)$  (with  $x_0^\gamma \in \Gamma \cap \mathcal{I}_0$ ) is nonzero, i.e.,

$$\hat{f}^\Gamma \triangleq \frac{1}{T_0} \int_0^{T_0} f^\Gamma(t) e^{-i\omega_0 t} dt \neq 0.$$

Then, a unique level set of the Fourier average  $f_{\omega_0}^*$  corresponds to a unique isochron. That is,  $f_{\omega_0}^*(x) = f_{\omega_0}^*(x^\gamma)$ , with

$x \in \mathcal{I}_\theta$  and  $x' \in \mathcal{I}_{\theta'}$ , if and only if  $\theta = \theta'$ . In addition,  $\theta - \theta' = \angle f_{\omega_0}^*(x) - \angle f_{\omega_0}^*(x')$  (where  $\angle$  denotes the argument of a complex number).

*Proof.* Given the definition of the isochron and the continuity of  $f$ , we have

$$\lim_{t \rightarrow \infty} |(f \circ \phi_t)(x) - f^\Gamma(t + \theta/\omega_0)| = 0 \tag{3}$$

for  $x \in \mathcal{I}_\theta$ . Then, it follows from Eqs. (2) and (3) that

$$\begin{aligned} & \left| f_{\omega_0}^*(x) - \frac{1}{T_0} \int_0^{T_0} f^\Gamma(t + \theta/\omega_0) e^{-i\omega_0 t} dt \right| \\ &= \left| \lim_{T \rightarrow \infty} \frac{1}{T} \int_0^T \left( (f \circ \phi_t)(x) - f^\Gamma(t + \theta/\omega_0) \right) e^{-i\omega_0 t} dt \right| \\ &\leq \lim_{T \rightarrow \infty} \frac{1}{T} \int_0^T \left| (f \circ \phi_t)(x) - f^\Gamma(t + \theta/\omega_0) \right| dt = 0, \end{aligned}$$

where the last equality holds since the integrand is bounded. Then, one has

$$f_{\omega_0}^*(x) = \frac{1}{T_0} \int_0^{T_0} f^\Gamma(t + \theta/\omega_0) e^{-i\omega_0 t} dt \tag{4}$$

or equivalently

$$f_{\omega_0}^*(x) = \hat{f}^\Gamma e^{i\theta} \quad \text{and} \quad f_{\omega_0}^*(x') = \hat{f}^\Gamma e^{i\theta'}$$

Since  $\hat{f}^\Gamma \neq 0$ , it follows that  $f_{\omega_0}^*(x) = f_{\omega_0}^*(x')$  if and only if  $\theta = \theta'$  and that  $\angle f_{\omega_0}^*(x) - \angle f_{\omega_0}^*(x') = \theta - \theta'$ , which completes the proof.  $\square$

*Remark 1.* Proposition 1 requires that the first Fourier coefficient  $\hat{f}^\Gamma$  of  $f^\Gamma$  be nonzero. However, an observable that satisfies  $\hat{f}^\Gamma = 0$  is not a generic function, so that Proposition 1 applies to almost all observables within the set of all possible functions.

*Remark 2.* Note that the complex Koopman eigenfunction  $z(x) = f_{k\omega_0}^*(x)$  satisfies  $|f_{k\omega_0}^*(x)| = c$  (with  $c$  constant) and also  $\dot{z} = ik\omega_0 z$ . This represents a rotation on a circle in a complex plane with angular speed  $\omega_0$ . Thus,  $z$  is a factor map<sup>10,21</sup>  $z : \mathcal{B}(\Gamma) \rightarrow \mathcal{C}$ , where  $\mathcal{C}$  is a circle of radius  $c$  that can be made  $\mathbb{S}^1$  by rescaling  $z$ .

### C. A new method for computing isochrons

Given the results of the previous section, we propose a new algorithm for computing the global isochrons of limit cycles, which relies on the evaluation of the Fourier averages. First, the Fourier averages (Eq. (2)) are (approximately) computed over a finite time horizon for a set of sample points in the state space. Then, the levels sets of the (finite time) Fourier averages are obtained through interpolation techniques and correspond to the isochrons.

We notice that (1) the method is particularly well-suited to the computation of isochrons in high-dimensional spaces and (2) the approximate Fourier averages are characterized by a good rate of convergence.

### 1. High-dimensional spaces

Standard methods cannot efficiently compute (global) isochrons in high-dimensional spaces. For instance, the use of standard backward integration methods is prohibited by numerical instability and sensitivity issues. In contrast, the computation of the Fourier averages only requires a forward integration and is therefore not limited by numerical issues, even for high dimensions. Moreover, the computation in high dimensional spaces is compatible with the use of Monte Carlo techniques (randomly distributed points) or adaptive grids. In particular, the points can be distributed only in selected regions (or subspaces) of interest or with a higher probability in regions characterized by more complex dynamics (see, e.g., the Hodgkin-Huxley model in Sec. III C).

### 2. Rate of convergence of the Fourier averages

The computation of the Fourier averages (Eq. (2)) is not numerically expensive. Provided that the limit cycle is exponentially stable, approximate Fourier averages obtained over finite time horizons  $T < \infty$  are characterized by a good rate of convergence. The approximation error is given by

$$\begin{aligned} & \left| f_{\omega_0}^*(x) - \frac{1}{T} \int_0^T (f \circ \phi_t)(x) e^{-i\omega_0 t} dt \right| \\ &\leq \left| f_{\omega_0}^*(x) - \frac{1}{T} \int_0^T f^\Gamma(t + \theta/\omega_0) e^{-i\omega_0 t} dt \right| \\ &+ \left| \frac{1}{T} \int_0^T \left( f^\Gamma(t + \theta/\omega_0) - (f \circ \phi_t)(x) \right) e^{-i\omega_0 t} dt \right|. \end{aligned} \tag{5}$$

Next, we introduce the values  $n \in \mathbb{N}$  and  $T' \in [0, T_0]$  so that  $T = nT_0 + T'$ . Then, it follows from Eq. (4) that the first term in the right hand of Eq. (5) yields

$$\begin{aligned} & \left| f_{\omega_0}^*(x) - \frac{1}{T} \int_0^T f^\Gamma(t + \theta/\omega_0) e^{-i\omega_0 t} dt \right| \\ &\leq \left| f_{\omega_0}^*(x) - \frac{1}{T} \left( nT_0 f_{\omega_0}^*(x) + \int_{nT_0}^{nT_0+T'} f^\Gamma(t + \theta/\omega_0) e^{-i\omega_0 t} dt \right) \right| \\ &\leq \frac{T - nT_0}{T} |f_{\omega_0}^*(x)| + \frac{T'}{T} \max_t |f^\Gamma(t)| \\ &\leq \frac{T_0}{T} \left( |f_{\omega_0}^*(x)| + \max_{x' \in \Gamma} |f(x')| \right). \end{aligned}$$

Since the limit cycle is exponentially stable, one has

$$|\phi(t, x) - \phi(t + \theta/\omega_0, x_0^*)| \leq C_1 e^{-C_2 t} \quad C_1, C_2 > 0$$

and the mean value theorem implies

$$\begin{aligned} & |f \circ \phi_t(x) - f^\Gamma(t + \theta/\omega_0)| \\ &\leq \max_{x \in \mathcal{B}(\Gamma)} |f'(x)| |\phi(t, x) - \phi(t + \theta/\omega_0, x_0^*)| \\ &\leq \max_{x \in \mathcal{B}(\Gamma)} |f'(x)| C_1 e^{-C_2 t}. \end{aligned}$$

Then, the second term in the right hand of Eq. (5) becomes

$$\begin{aligned} & \left| \frac{1}{T} \int_0^T \left( f^\Gamma(t + \theta/\omega_0) - (f \circ \phi_t)(x) \right) e^{-i\omega_0 t} dt \right| \\ & \leq \frac{1}{T} \int_0^T |f^\Gamma(t + \theta/\omega_0) - (f \circ \phi_t)(x)| dt \\ & \leq \frac{C_1 \max_{x \in B(\Gamma)} |f'(x)|}{T} \int_0^T e^{-C_2 t} dt \\ & \leq \frac{C_1 \max_{x \in B(\Gamma)} |f'(x)|}{C_2 T} (1 - e^{-C_2 T}) \leq \frac{C_1 \max_{x \in B(\Gamma)} |f'(x)|}{C_2 T}. \end{aligned}$$

Finally, the estimation error for the Fourier average is bounded by

$$\begin{aligned} & \left| f_{\omega_0}^*(x) - \frac{1}{T} \int_0^T (f \circ \phi_t)(x) e^{-i\omega_0 t} dt \right| \\ & \leq \frac{T_0 \left( |f_{\omega_0}^*(x)| + \max_{x' \in \Gamma} |f'(x')| \right) + \frac{C_1}{C_2} \max_{x \in B(\Gamma)} |f'(x)|}{T}. \end{aligned}$$

Since the Fourier averages converge with the rate  $T^{-1}$ , the isochrons are obtained over reasonably short time horizons.

### III. APPLICATIONS

In this section, we present several examples of increasing complexity, which show that the new method is efficient to compute the isochrons of limit cycles. For each example, the results are compared with other methods or known results.

#### A. A trivial example

We first consider a model for which the (trivial) analytical expression of the isochrons is known. Namely, we consider the first order system with periodic forcing

$$\dot{x} = -\lambda x + \sin(\omega t + \theta_0) \quad x \in \mathbb{R}, \quad (6)$$

which can be rewritten as a nonlinear autonomous system

$$\dot{x} = -\lambda x + \sin(\theta), \quad \dot{\theta} = \omega \quad (7)$$

with  $(x, \theta) \in \mathbb{R} \times \mathbb{S}^1$  and  $\theta(0) = \theta_0$ . It is well-known that, for any initial condition, the solution of Eq. (6) asymptotically converges to  $x(t) = A \sin(\omega t + \theta_0 + \varphi)$ , where  $A$  and  $\varphi$  depend only on the frequency  $\omega$ . Since the solution of Eq. (7) satisfies  $\theta(t) = \omega t + \theta_0$ , the system has a globally attractive limit cycle  $x = A \sin(\theta + \varphi)$ , with a frequency  $\omega_0 = \omega$ . In addition, the isochrons are simply given by  $\mathcal{I}_{\theta_0} = \{(x, \theta) | \theta = \theta_0\}$ , so that they do not depend on  $x$ .

Figure 1 shows that the Fourier averages computed for the system Eq. (7) are independent of the variable  $x$ . The level sets of the Fourier averages therefore correspond to the isochrons of the limit cycle. It is noticeable that the chosen observable  $f(x, \theta) = x$ , which depends only on  $x$ , is sufficient to compute the isochrons, which are themselves independent of  $x$ . This is due to the fact that the dynamics of  $x$  is affected by the dynamics of  $\theta$ .

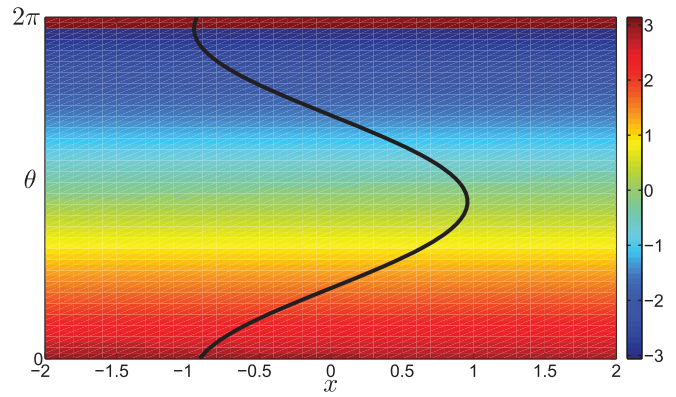


FIG. 1. Argument  $\angle f_{\omega_0}^*$  of the Fourier average of the observable  $f(x, \theta) = x$  (computed on a grid  $40 \times 60$ ,  $\omega_0 = 1$ ). The black curve is the limit cycle in  $\mathbb{R} \times \mathbb{S}^1$ .

#### B. The Van der Pol model

Now, we consider the classical Van der Pol oscillator model

$$\dot{x}_1 = x_2, \quad \dot{x}_2 = \mu(1 - x_1^2)x_2 - x_1,$$

with the parameter  $\mu = 0.3$  (the frequency is  $\omega_0 \approx 0.995$ ). In Figure 2, the isochrons are computed with a standard backward integration technique and with the Fourier averages. The results are in good agreement and emphasize the validity of the new method.

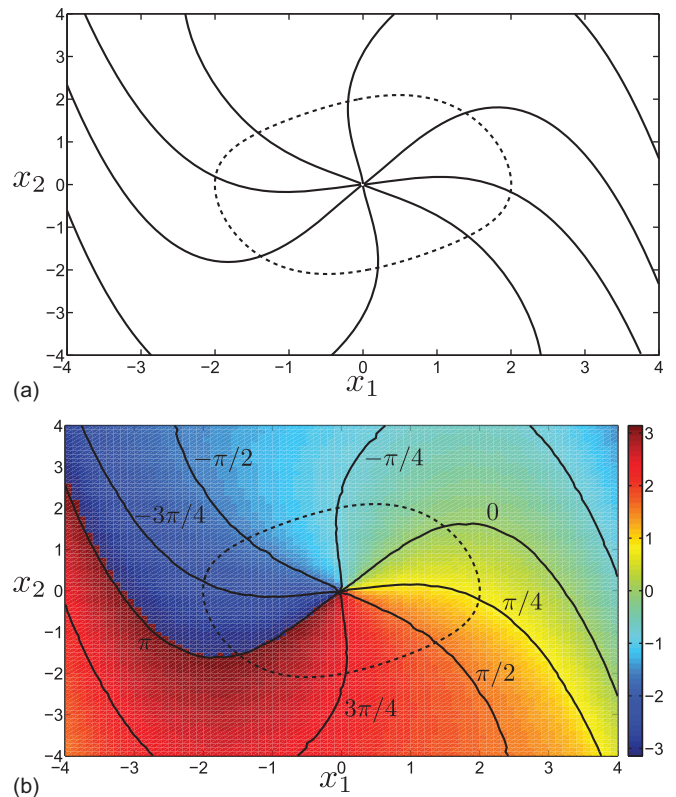


FIG. 2. (a) The isochrons of the Van der Pol oscillator are computed with a standard backward integration technique. (b) The isochrons are the level sets (solid curves) of the Fourier average of the observable  $f(x_1, x_2) = x_1 + x_2$ . The color represents the argument  $\angle f_{\omega_0}^*$  (computed on a grid  $80 \times 80$ ) (the dashed orbit is the limit cycle).

### C. The (high-dimensional) Hodgkin-Huxley model

The 4-dimensional Hodgkin-Huxley model,<sup>4</sup> which is probably the most popular model in neuroscience, can admit a limit cycle (see the appendix for the equations and parameters). However, since this limit cycle is characterized by a non-planar slow-fast dynamics, it is difficult to compute the global isochrons through standard methods. In contrast, the Fourier averages of an observable are easily obtained, in spite of the slow-fast multidimensional dynamics, and provide a straightforward framework to compute the isochrons of the Hodgkin-Huxley model.

Figure 3 shows the intersections of the isochrons with the 3-dimensional subspace  $h + n = 0.8$  (the limit cycle lies—in good approximation—in the subspace  $h + n = 0.8$ ). It is noticeable that the accuracy has been increased—with a higher distribution probability of the sample points—in regions of high concentration of isochrons.

The results are consistent with the isochrons of the 2-dimensional reduction of the Hodgkin-Huxley model.<sup>7</sup> In particular, the isochrons are independent of the variables  $V$  and  $m$ , when far from the limit cycle, an observation explained by the two time scales of the system (the variables  $V$  and  $m$  are fast with respect to  $n$  and  $h$ ). In addition, the validity of the results is also emphasized by Fig. 4, which shows that two trajectories with an initial condition on the same isochron eventually converge toward the same orbit on the limit cycle.

### IV. GENERALIZED ISOCHRONS OF THE TWO-DIMENSIONAL TORUS

In contrast to periodic motions on a limit cycle, quasiperiodic oscillations on a torus involve two (or more) basic frequencies. Computing the Fourier averages for several frequencies therefore appears as a natural extension of the above framework to quasiperiodic oscillations and motivates the introduction of *generalized isochrons* that lead to a phase parametrization of the basin of attraction. Provided that the generalized isochrons exist (i.e., that phase coordinates are well-defined), their intersections correspond to the fibers of the stable manifold of the torus.

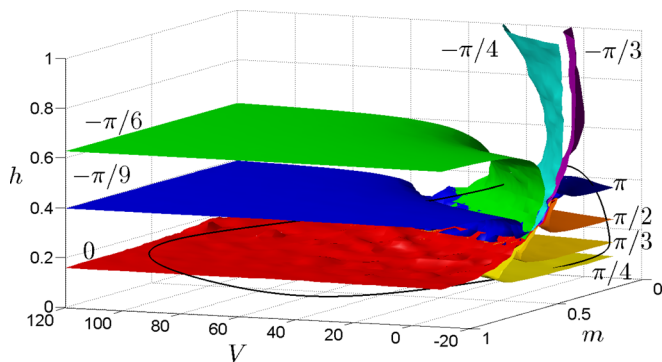


FIG. 3. The isochrons of the Hodgkin-Huxley model are obtained by computing the level sets of the Fourier averages of  $f(V, m, h, n) = m$ . The figure shows the intersection of several isochrons with the subspace  $h + n = 0.8$ . The black orbit is the projection of the limit cycle in the subspace (the Fourier averages are computed over a finite time horizon  $T = 300$  for 30 000 points distributed in the subspace, with a higher probability in regions characterized by a high concentration of isochrons).

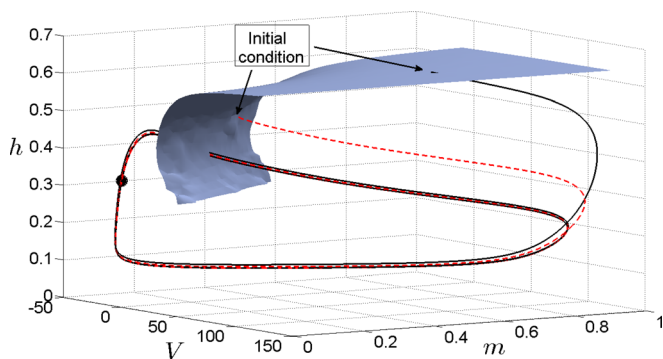


FIG. 4. The two trajectories (dashed red and solid black curves) have an initial condition that belongs to the same isochron  $\mathcal{I}_\theta$ , with  $\theta = -\pi/6$ . They eventually approach the same orbit on the limit cycle (the initial condition is (6.018, 0.3077, 0.4974, 0.3026) for the dashed red trajectory and (73.33, 0.641, 0.6235, 0.1765) for the solid black trajectory. After a time  $t = 50$ , the dashed red trajectory reaches the point  $(-6.238, 0.024, 0.334, 0.503)$  and the solid black trajectory reaches the point  $(-6.255, 0.024, 0.333, 0.503)$  (black dot).

### A. Generalized isochrons

Let us consider a dynamical system

$$\dot{x} = F(x) \quad x \in \mathbb{R}^n \tag{8}$$

which admits a stable quasiperiodic attractor  $\Gamma$ , with a basin of attraction  $\mathcal{B}(\Gamma) \subseteq \mathbb{R}^n$ . In addition, we let  $\phi : \mathbb{R}^+ \times \mathbb{R}^n \mapsto \mathbb{R}^n$  denote the flow induced by Eq. (8).

For the sake of simplicity, we assume that the attractor  $\Gamma$  is a two-dimensional torus: the quasiperiodic oscillations of a trajectory on  $\Gamma$  depend on the two incommensurable frequencies  $\omega_1$  and  $\omega_2$  (i.e., the rotation number  $\omega_1/\omega_2$  is irrational). Typically, such a dynamical system can be obtained with two interacting systems of independent natural frequencies (e.g., two coupled Van der Pol oscillators, see Sec. IV C). It is noticeable that there is no loss of generality with the above assumption, since the developments presented in the sequel are easily extended to quasiperiodic motions involving more than two frequencies.

For a periodic system (of period  $T_0$ ), the subsets of the attractor that are invariant under the time- $T_0$  map  $\phi(T_0, \cdot)$  correspond to single points. In contrast, for a quasiperiodic system, the subsets of the attractor that are invariant under the maps  $\phi(T_1, \cdot)$  and  $\phi(T_2, \cdot)$  (with  $T_1 = 2\pi/\omega_1$  and  $T_2 = 2\pi/\omega_2$ ) are not single points. These sets are defined as follows:

*Definition 2.* For  $j = \{1, 2\}$ , the set  $\gamma_{\theta_j}$  associated with the phase  $\theta_j \in \mathbb{S}^1$  is defined by

$$\gamma_{\theta_j} = \overline{\bigcup_{k \in \mathbb{Z}} \phi((k + \theta_j/(2\pi))T_j, x_0^j)},$$

where “ $\overline{\phantom{x}}$ ” represents the closure of the set and where  $x_0^j \in \Gamma$  is an arbitrarily chosen point of the attractor which corresponds to the phases  $(\theta_1, \theta_2) = (0, 0)$ .

When the above definition leads to continuous curves, the curves  $\gamma_{\theta_1}$  and  $\gamma_{\theta_2}$  parametrize the (two-dimensional) torus  $\Gamma$  with phase coordinates: a point of  $\Gamma$  corresponds to the intersection  $\gamma_{\theta_1} \cap \gamma_{\theta_2}$  and is thereby associated with the

unique pair  $(\theta_1, \theta_2)$ . In addition, the dynamics Eq. (8) on  $\Gamma$  is turned into the phase dynamics

$$\dot{\theta}_1 = \omega_1, \quad \dot{\theta}_2 = \omega_2 \tag{9}$$

on the standard torus  $\mathbb{T}^2 = \mathbb{S}^1 \times \mathbb{S}^1$ .

*Remark 3.* The sets  $\gamma_{\theta_j}$  of Definition 2 may fail to be continuous curves and a phase parametrization of the torus may not exist. More precisely, the existence of factor maps that map  $\Gamma$  to the standard torus  $\mathbb{T}^2$  is not always guaranteed (this corresponds to the existence of a solution for the so-called *invariant equation*<sup>15</sup>). However, results from KAM theory ensure the existence of phase coordinates provided that the rotation number  $\omega_1/\omega_2$  is Diophantine (see, e.g., Sec. III in Ref. 1). In this case, the flow on  $\Gamma$  is diffeomorphic to the parallel flow Eq. (9) on  $\mathbb{T}^2$ , and it is clear that a trajectory of the map  $\phi(T_j, \cdot)$  densely fills a (closed) curve  $\gamma_j$  on  $\Gamma$ . In the sequel, we therefore restrict the discussion to this situation, which is generic since the set of Diophantine numbers is of measure one (the results are similar in higher dimensions: Definition 2 is still valid provided that the rotation vector  $(\omega_1, \dots, \omega_n)$  satisfies the so-called *Diophantine condition*<sup>1</sup>).

Next, we define two families of  $(n - 1)$ -dimensional *generalized isochrons* that extend the phase characterization to the whole basin of attraction  $\mathcal{B}(\Gamma)$ .

*Definition 3.* For  $j = \{1, 2\}$ , the generalized isochron  $\mathcal{I}_{\theta_j}$ —associated with the phase  $\theta_j \in [0, 2\pi)$ —of the attractor  $\Gamma$  is the  $(n - 1)$ -dimensional manifold defined as

$$\mathcal{I}_{\theta_j} = \{x \in \mathcal{B}(\Gamma) | \exists x^j \in \gamma_{\theta_j} \text{ s.t. } \lim_{t \rightarrow \infty} \|\phi(t, x) - \phi(t, x^j)\| = 0\}.$$

*Remark 4.* When phase coordinates are well-defined on the torus (see Remark 3), the existence of the generalized isochrons as  $(n - 1)$ -dimensional manifolds is ensured provided that the attractor is a normally hyperbolic manifold. Indeed, a curve  $\gamma_{\theta_j}$  is a normally hyperbolic invariant manifold for the time- $T_j$  map  $\phi(T_j, \cdot)$  and it follows from Definition 3 that the generalized isochron  $\mathcal{I}_{\theta_j}$  is the invariant stable set of  $\gamma_{\theta_j}$ . Then, invariant manifold theory implies that the generalized isochron is a manifold.<sup>3,22</sup>

The generalized isochrons characterize the asymptotic behavior of the quasiperiodic trajectories. Two trajectories with an initial condition on the same isochron  $\mathcal{I}_{\theta_j}$  eventually converge to the same curve  $\gamma_{\theta_j + \omega_j t}$  on  $\Gamma$ . Furthermore, two trajectories with an initial condition on the same intersection of the two isochrons  $\mathcal{I}_{\theta_1}$  and  $\mathcal{I}_{\theta_2}$  eventually converge to the same intersection of  $\gamma_{\theta_1 + \omega_1 t}$  and  $\gamma_{\theta_2 + \omega_2 t}$  on  $\Gamma$ , that is, to the *same trajectory*. This motivates the following definition.

*Definition 4.* The  $(n - 2)$ -dimensional manifold  $\mathcal{I}_{(\theta_1, \theta_2)}$  associated with the phases  $(\theta_1, \theta_2)$  is defined by

$$\begin{aligned} \mathcal{I}_{(\theta_1, \theta_2)} &\triangleq \mathcal{I}_{\theta_1} \cap \mathcal{I}_{\theta_2} \\ &= \{x \in \mathcal{B}(\Gamma) | \lim_{t \rightarrow \infty} \|\phi(t, x) - \phi(t, x^j)\| = 0\}, \end{aligned}$$

with  $x^j = \gamma_{\theta_1} \cap \gamma_{\theta_2}$ .

The intersections  $\mathcal{I}_{(\theta_1, \theta_2)}$  are conceptually related to the isochrons  $\mathcal{I}_{\theta}$  of a limit cycle: both are fibers of the stable manifold of the attractor (limit cycle or torus). Since they are associated with a unique point of the attractor, they play a key role in studies of synchronization of trajectories.

*Remark 5.* It is important to note that the definition of isochrons (Definition 3 and Definition 4) comes along with the introduction of phase coordinates on the attractor. While invariant manifold theory implies that stable manifolds of hyperbolic invariant manifolds can always be invariantly fibered,<sup>3,22</sup> the existence of phase coordinates (and thus the existence of isochrons of Definition 3 and Definition 4) is not always guaranteed (see Remark 3).

### B. Fourier averages

As in the periodic case, the Fourier averages (Eq. (2)) provide a simple and straightforward framework to obtain the generalized isochrons of the (two-dimensional) torus. Namely, the level sets of the Fourier averages  $f_{\omega_1}^*$  and  $f_{\omega_2}^*$  are invariant under the time- $T_1$  map  $\phi(T_1, \cdot)$  and the time- $T_2$  map  $\phi(T_2, \cdot)$ , respectively. They therefore correspond to the generalized isochrons of Definition 3.

*Proposition 2.* Let  $j = \{1, 2\}$  and consider an observable  $f \in C^1$  such that

$$\hat{f}_{\omega_j}^\Gamma \triangleq \lim_{T \rightarrow \infty} \frac{1}{T} \int_0^T f^\Gamma(t) e^{-i\omega_j t} dt \neq 0,$$

where  $f^\Gamma(t) \triangleq (f \circ \phi_t)(x_0^j)$  (with  $x_0^j = \mathcal{I}_{(0,0)} \cap \Gamma$ ). Then, a unique level set of the Fourier average  $f_{\omega_j}^*$  corresponds to a unique generalized isochron  $\mathcal{I}_{\theta_j}$ . That is,  $f_{\omega_j}^*(x) = f_{\omega_j}^*(x')$ , with  $x \in \mathcal{I}_{\theta_j}$  and  $x' \in \mathcal{I}_{\theta_j'}$ , if and only if  $\theta_j = \theta_j'$ . In addition,  $\theta_j - \theta_j' = \angle f_{\omega_j}^*(x) - \angle f_{\omega_j}^*(x')$ .

*Proof.* Given Definition 2 and Definition 3, if  $x$  belongs to the generalized isochron  $\mathcal{I}_{\theta_j}$ , then for all  $\epsilon > 0$ , there exists  $k \in \mathbb{Z}$  such that

$$\lim_{t \rightarrow \infty} \|\phi(t, x) - \phi(t + k 2\pi/\omega_j + \theta_j/\omega_j, x_0^j)\| < \epsilon$$

or, since  $f \in C^1$ , there exists  $k \in \mathbb{Z}$  such that

$$\lim_{t \rightarrow \infty} |(f \circ \phi_t)(x) - f^\Gamma(t + k 2\pi/\omega_j + \theta_j/\omega_j)| < \epsilon. \tag{10}$$

Then, it follows from Eqs. (2) and (10) that

$$\begin{aligned} &\left| f_{\omega_j}^*(x) - \lim_{T \rightarrow \infty} \frac{1}{T} \int_0^T f^\Gamma(t + \theta_j/\omega_j) e^{-i\omega_j t} dt \right| \\ &= \left| \lim_{T \rightarrow \infty} \frac{1}{T} \int_0^T (f \circ \phi_t)(x) e^{-i\omega_j t} dt \right. \\ &\quad \left. - \lim_{T \rightarrow \infty} \frac{1}{T} \int_0^T f^\Gamma(t + k 2\pi/\omega_j + \theta_j/\omega_j) e^{-i\omega_j t} dt \right| \\ &\leq \lim_{T \rightarrow \infty} \frac{1}{T} \int_0^T \left| (f \circ \phi_t)(x) - f^\Gamma(t + k 2\pi/\omega_j + \theta_j/\omega_j) \right| dt < \epsilon, \end{aligned} \tag{11}$$

where the last inequality holds since the integrand is bounded. Since the constant  $\epsilon$  (which depends on  $k$ ) can be

arbitrarily small, the left hand side of Eq. (11) (which does not depend on  $k$ ) is equal to zero. Then, one has

$$f_{\omega_j}^*(x) = \lim_{T \rightarrow \infty} \frac{1}{T} \int_0^T f^\Gamma(t + \theta_j/\omega_j) e^{-i\omega_j t} dt$$

or equivalently

$$f_{\omega_j}^*(x) = \hat{f}_{\omega_j}^\Gamma e^{i\theta_j} \quad \text{and} \quad f_{\omega_j}^*(x') = \hat{f}_{\omega_j}^\Gamma e^{i\theta_j'}$$

Since  $\hat{f}_{\omega_j}^\Gamma \neq 0$ , it follows that  $f_{\omega_j}^*(x) = f_{\omega_j}^*(x')$  if and only if  $\theta_j = \theta_j'$  and that  $\angle f_{\omega_j}^*(x) - \angle f_{\omega_j}^*(x') = \theta_j - \theta_j'$ , which completes the proof.  $\square$

Proposition 2 implies that the method described in Sec. II C can be used to compute not only the isochrons of the limit cycle but also the generalized isochrons of the torus. For the computation of generalized isochrons, the method is particularly well-suited given the high dimension of the system ( $n \geq 3$ ). It contrasts with standard backward integration techniques that are difficult to use since the trajectories starting from a generalized isochron converge to a one-dimensional set of the attractor (and not to a single point). In addition, the computation of the Fourier averages is characterized by a rate of convergence that is as good as in the periodic case (Sec. II C).

### C. Example: Two coupled Van der Pol oscillators

We use the method of the Fourier averages to compute the generalized isochrons of two coupled Van der Pol oscillators

$$\begin{aligned} \dot{x}_1 &= x_2, & \dot{x}_2 &= \mu(1 - x_1^2)x_2 - k_x x_1 + k_c(y_1 - x_1), \\ \dot{y}_1 &= y_2, & \dot{y}_2 &= \mu(1 - y_1^2)y_2 - k_y y_1 + k_c(x_1 - y_1). \end{aligned} \quad (12)$$

With the parameters  $\mu = 0.3$ ,  $k_x = 1$ ,  $k_y = 3$ , and  $k_c = 0.5$ , the two coupled oscillators are in quasiperiodic regime (the basic frequencies of the quasiperiodic oscillations are  $\omega_1 \approx 1.1741$  and  $\omega_2 \approx 1.8944$ ). We adopt these parameters in the sequel.

The frequency  $\omega_1$  (resp.  $\omega_2$ ) is associated with the first oscillator (resp. the second oscillator). It follows that the generalized isochrons, say  $\mathcal{I}_{\theta_1}$ , depend strongly on the variables  $x_1$  and  $x_2$ , while their dependence on the two other variables is only induced by the coupling. In particular, with no coupling, the generalized isochrons  $\mathcal{I}_{\theta_1}$  are independent of  $y_1$  and  $y_2$ .

#### 1. On the attractor

First, the Fourier averages  $f_{\omega_1}^*$  and  $f_{\omega_2}^*$ —of the observable  $f(x_1, x_2, y_1, y_2) = x_1 + y_1$ —are computed on the attractor  $\Gamma$  of Eq. (12) (Fig. 5). Their level sets correspond to the curves  $\gamma_{\theta_1}$  and  $\gamma_{\theta_2}$ , respectively.

#### 2. Generalized isochrons $\mathcal{I}_{\theta_1}$

The level sets of the Fourier averages  $f_{\omega_1}^*$  are now computed in the entire 4-dimensional state space. They correspond to the generalized isochrons  $\mathcal{I}_{\theta_1}$  (similar results,

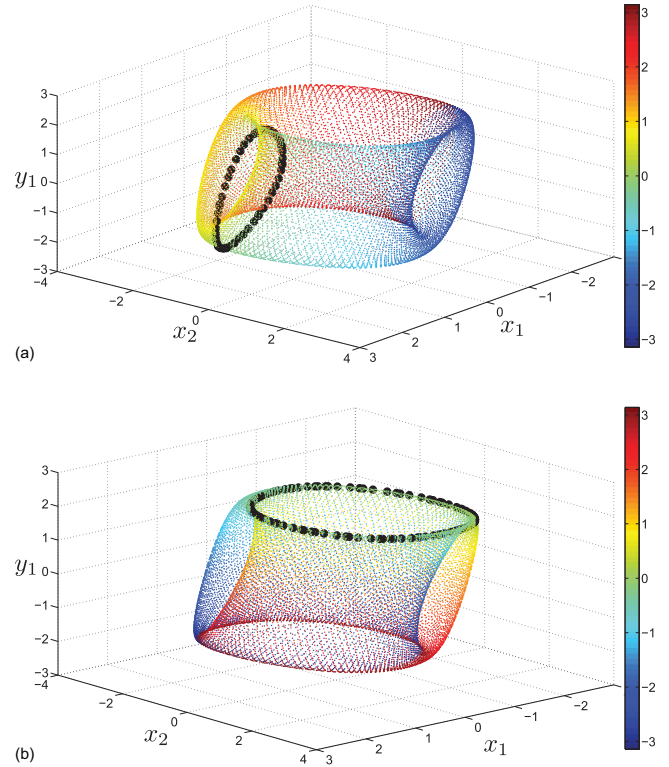


FIG. 5. (a) The level sets of  $f_{\omega_1}^*$  on the attractor correspond to the curves  $\gamma_{\theta_1}$ . The black dots represent the curve corresponding to the phase  $\theta_1 = 0$ . (b) Idem with  $f_{\omega_2}^*$  for the curves  $\gamma_{\theta_2}$  (the Fourier averages are computed for the observable  $f(x_1, x_2, y_1, y_2) = x_1 + y_1$  and the attractor is projected in the 3-dimensional subspace  $y_2 = 0$ ).

which are obtained for the Fourier averages  $f_{\omega_2}^*$  and the generalized isochrons  $\mathcal{I}_{\theta_2}$ , are not shown).

Figures 6 and 7 show the (2-dimensional) surfaces which correspond to the intersections of the (3-dimensional) generalized isochrons  $\mathcal{I}_{\theta_1}$  with the 3-dimensional subspace  $y_2 = 0$ . Figure 8 shows the intersections of the same generalized isochrons, but with the 3-dimensional subspace  $x_2 = 0$ . (the intersections of the 2-dimensional surfaces with the attractor do not correspond to the curves  $\gamma_{\theta_1}$ , since the attractor is projected in the subspace).

It is remarkable that the generalized isochrons  $\mathcal{I}_{\theta_1}$  are (almost) independent of  $y_2$  (see Fig. 8). This observation can

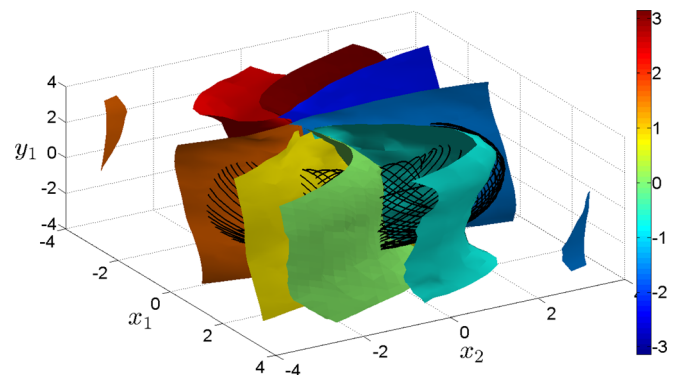


FIG. 6. Intersections of the generalized isochrons  $\mathcal{I}_{\theta_1}$  ( $\theta_1 = k\pi/4$ ,  $k \in \mathbb{Z}$ ) with the 3-dimensional subspace  $y_2 = 0$ . The black orbit is the attractor (the Fourier averages of the observable  $f(x_1, x_2, y_1, y_2) = x_1 + y_1$  are computed over a finite time horizon  $T = 200$  for 20 000 points (randomly distributed)).

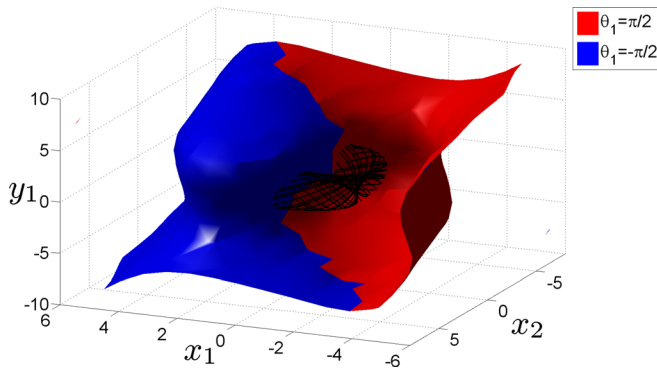


FIG. 7. Detailed view of the intersection of two generalized isochrons  $\mathcal{I}_{\theta_1}$  ( $\theta_1 = \pm\pi/2$ ) with the subspace  $y_2 = 0$  (the Fourier averages of the observable  $f(x_1, x_2, y_1, y_2) = x_1 + y_1$  are computed over a finite time horizon  $T = 200$  on a grid  $13 \times 13 \times 13 \times 13$ ).

be explained by the fact that the dynamics Eq. (12) of the first oscillator depend on the variables  $x_1, x_2$ , and  $y_1$  (through the coupling), but do not (directly) depend on  $y_2$ .

**3. Intersections of generalized isochrons  $\mathcal{I}_{(\theta_1, \theta_2)}$**

We can finally compute the intersection  $\mathcal{I}_{(\theta_1, \theta_2)}$  of the generalized isochrons  $\mathcal{I}_{\theta_1}$  and  $\mathcal{I}_{\theta_2}$ . Figure 9 displays two generalized isochrons  $\mathcal{I}_{\theta_1}$  and two generalized isochrons  $\mathcal{I}_{\theta_2}$ . Their intersections correspond to four (connected) curves which represent the intersection of  $\mathcal{I}_{(\theta_1, \theta_2)}$  with the subspace  $x_2 = 0$ . One verifies that two trajectories with an initial condition on the same intersection  $\mathcal{I}_{(\theta_1, \theta_2)}$  eventually converge to the same orbit on the torus (see Fig. 10).

**V. CONCLUSION**

In this paper, we proposed a novel method for computing the global isochrons of high-dimensional systems: the isochrons are computed as the level sets of (Fourier) time averages evaluated along the trajectories. The method is supported by theoretical results and is related to spectral properties of the Koopman semigroup associated with the underlying ordinary differential equations. In addition, the evaluation of the Fourier averages is characterized by a good rate of convergence. More importantly, while the usual

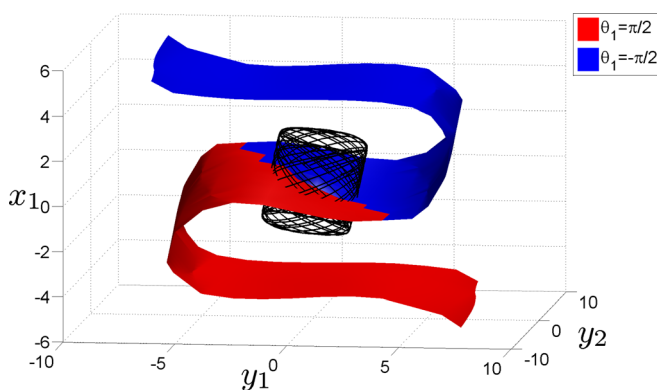


FIG. 8. Intersections of two generalized isochrons  $\mathcal{I}_{\theta_1}$  ( $\theta_1 = \pm\pi/2$ ) with the 3-dimensional subspace  $x_2 = 0$  (the Fourier averages of the observable  $f(x_1, x_2, y_1, y_2) = x_1 + y_1$  are computed over a finite time horizon  $T = 200$  on a grid  $13 \times 13 \times 13 \times 13$ ).

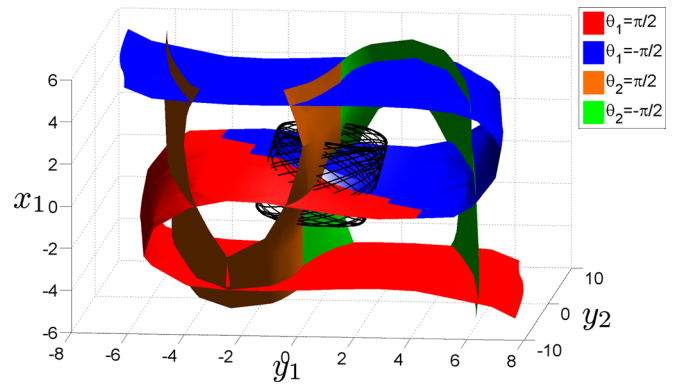


FIG. 9. The intersection of the generalized isochrons  $\mathcal{I}_{\theta_1}$  and  $\mathcal{I}_{\theta_2}$  ( $\theta_1 = \pm\pi/2, \theta_2 = \pm\pi/2$ ) corresponds to  $\mathcal{I}_{(\theta_1, \theta_2)}$  (in the subspace  $x_2 = 0$ ) (the Fourier averages of the observable  $f(x_1, x_2, y_1, y_2) = x_1 + y_1$  are computed over a finite time horizon  $T = 200$  on a grid  $13 \times 13 \times 13 \times 13$ ).

(backward integration) methods are restricted to computations in two-dimensional spaces, our new (forward integration) method is a convenient and flexible method to obtain global isochrons in high-dimensional spaces.

Since the method relies on a general background, it is not restricted to asymptotically periodic systems. In the case of quasiperiodic systems, the computation of the Fourier averages for several basic frequencies appears as a natural extension of the method and leads to the definition of generalized isochrons of the torus. This framework extends the notion of phase sensitivity to quasiperiodic dynamics, potentially opening new research perspectives such as the study of populations of interacting quasiperiodic systems.

Existence (and persistence under small perturbations) of generalized isochrons could be shown by the contraction mapping principle. An interesting technical difficulty is that the KAM-type results would need to be used to prove the Diophantine nature of the perturbed torus flow, and this is typically possible only for a Cantor set of parametrized perturbations in the current case. However, it would be an interesting coupling of KAM theory and normally hyperbolic invariant manifold theory.

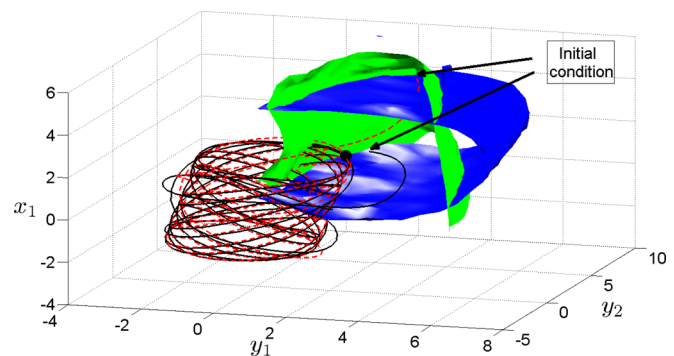


FIG. 10. The two trajectories (dashed red and solid black curves) have an initial condition that belongs to the same generalized isochrons  $\mathcal{I}_{\theta_1}$  (blue) and  $\mathcal{I}_{\theta_2}$  (green), with  $\theta_1 = \theta_2 = -\pi/2$ . They eventually approach the same orbit on the torus (the initial condition is  $(4.294, 0, 2.5, 6.5)$  for the dashed red trajectory and  $(0.5, 0, 1.5, 9.153)$  for the solid black trajectory. After a time  $t = 60$ , the dashed red trajectory reaches the point  $(1.506, -0.224, 1.690, 3.080)$  and the solid black trajectory reaches the point  $(1.511, -0.315, 1.713, 3.028)$  (black dot).



## ACKNOWLEDGMENTS

A. Mauroy holds a postdoctoral fellowship from the Belgian American Educational Foundation. This work was partially funded by Army Research Office Grant W911NF-11-1-0511, with Program Manager Dr. Sam Stanton.

## APPENDIX A: HODGKIN-HUXLEY MODEL

The Hodgkin-Huxley model is characterized by the 4-dimensional dynamics (voltage  $V$  and gating variables  $m$ ,  $h$ ,  $n$  for the (in)activation of the ions channels  $\text{Na}^+$  and  $\text{K}^+$ )

$$\begin{aligned}\dot{V} &= 1/C \left( -\bar{g}_{\text{Na}}(V - V_{\text{Na}})m^3h - \bar{g}_{\text{K}}(V - V_{\text{K}})n^4 \right. \\ &\quad \left. - g_{\text{L}}(V - V_{\text{L}}) + I_b \right), \\ \dot{m} &= \alpha_m(V)(1 - m) - \beta_m(V)m, \\ \dot{h} &= \alpha_h(V)(1 - h) - \beta_h(V)h, \\ \dot{n} &= \alpha_n(V)(1 - n) - \beta_n(V)n,\end{aligned}$$

with the functions

$$\begin{aligned}\alpha_m(V) &= (0.1V - 2.5)/[1 - \exp(2.5 - 0.1V)], \\ \beta_m(V) &= 4 \exp(-V/18), \\ \alpha_h(V) &= 0.07 \exp(-V/20), \\ \beta_h(V) &= 1/[1 + \exp(3 - 0.1V)], \\ \alpha_n(V) &= (0.01V - 0.1)/[1 - \exp(1 - 0.1V)], \\ \beta_n(V) &= 0.125 \exp(-V/80).\end{aligned}$$

In the present paper, we adopt the usual parameters

$$\begin{aligned}V_{\text{Na}} &= 115 \text{ mV}, \quad V_{\text{K}} = -12 \text{ mV}, \quad V_{\text{L}} = 10.6 \text{ mV}, \\ \bar{g}_{\text{Na}} &= 120 \text{ mS/cm}^2, \quad \bar{g}_{\text{K}} = 36 \text{ mS/cm}^2, \\ \bar{g}_{\text{L}} &= 0.3 \text{ mS/cm}^2, \quad C = 1 \text{ }\mu\text{F/cm}^2.\end{aligned}$$

With the bias current  $I_b = 10 \text{ mA}$ , the system admits a limit cycle characterized by a slow-fast dynamics (the frequency of the limit cycle is  $\omega_0 \approx 0.429$ ).

<sup>1</sup>R. de la Llave, in *Proceedings of Symposia in Pure Mathematics, Seattle, WA* (American Mathematical Society, 1999), Vol. 69.

- <sup>2</sup>A. Guillamon and G. Hugué, "A computational and geometric approach to phase resetting curves and surfaces," *SIAM J. Appl. Dyn. Syst.* **8**, 1005–1042 (2009).
- <sup>3</sup>M. W. Hirsch, C. C. Pugh, and M. Shub, *Invariant Manifolds*, Lecture Notes in Mathematics Vol. 583 (Springer-Verlag, 1977).
- <sup>4</sup>A. L. Hodgkin and A. F. Huxley, "A quantitative description of membrane current and its application to conduction and excitation in nerve," *Bull. Math. Biol.* **52**(1–2), 25–71 (1990).
- <sup>5</sup>F. C. Hoppensteadt and E. M. Izhikevich, *Weakly Connected Neural Networks* (Springer-Verlag, New York, 1997).
- <sup>6</sup>E. M. Izhikevich, *Dynamical Systems in Neuroscience: The Geometry of Excitability and Bursting* (MIT, 2007).
- <sup>7</sup>J. Keener and J. Sneyd, *Mathematical Physiology* (Springer-Verlag, New York, 1998).
- <sup>8</sup>I. G. Malkin, *The Methods of Lyapunov and Poincaré in the Theory of Nonlinear Oscillations* (Gostekhizdat, Moscow-Leningrad, 1949).
- <sup>9</sup>I. Mezic, "Spectral properties of dynamical systems, model reduction and decompositions," *Nonlinear Dyn.* **41**, 309–325 (2005).
- <sup>10</sup>I. Mezic and A. Banaszuk, "Comparison of systems with complex behavior," *Physica D* **197**, 101–133 (2004).
- <sup>11</sup>I. Mezic and S. Wiggins, "A method for visualization of invariant sets of dynamical systems based on the ergodic partition," *Chaos* **9**, 213–218 (1999).
- <sup>12</sup>H. M. Osinga and J. Moehlis, "Continuation-based computation of global isochrons," *SIAM J. Appl. Dyn. Syst.* **9**, 1201–1228 (2010).
- <sup>13</sup>K. Petersen, *Ergodic Theory* (Cambridge University Press, Cambridge, England, 1995).
- <sup>14</sup>P. Sacré and R. Sepulchre, in *Proceedings of the 50th IEEE Conference on Decision and Control*, 12–15 December 2011.
- <sup>15</sup>F. Schilder, H. Osinka, and W. Vogt, "Continuation of quasi-periodic invariant tori," *SIAM J. Appl. Dyn. Syst.* **4**, 459 (2005).
- <sup>16</sup>W. E. Sherwood and J. Guckenheimer, "Dissecting the phase response of a model bursting neuron," *SIAM J. Appl. Dyn. Syst.* **9**, 659–703 (2010).
- <sup>17</sup>S. H. Strogatz, "From Kuramoto to Crawford: Exploring the onset of synchronization in populations of coupled oscillators," *Physica D* **143**, 1–20 (2000).
- <sup>18</sup>O. Suvak and A. Demir, "Quadratic approximations for the isochrons of oscillators: A general theory, advanced numerical methods, and accurate phase computations," *IEEE Trans. Comput.-Aided Des.* **29**, 1215–1228 (2010).
- <sup>19</sup>D. Takeshita and R. Feres, "Higher order approximation of isochrons," *Nonlinearity* **23**, 1303–1323 (2010).
- <sup>20</sup>S. R. Taylor, R. Gunawan, L. R. Petzold, and F. J. Doyle, "Sensitivity measures for oscillating systems: Application to mammalian circadian gene network," *IEEE Trans. Autom. Control* **53**, 177–188 (2008).
- <sup>21</sup>T. Wichtrey, "Harmonic limits of dynamical systems," *Discrete Contin. Dyn. Syst. Supplement* 2011, 1432–1439 (2011).
- <sup>22</sup>S. Wiggins, *Normally Hyperbolic Invariant Manifolds in Dynamical Systems* (Springer, 1994), Vol. 105.
- <sup>23</sup>A. Winfree, *The Geometry of Biological Time*, 2nd ed. (Springer-Verlag, New York, 2001).
- <sup>24</sup>A. T. Winfree, "Patterns of phase compromise in biological cycles," *J. Math. Biol.* **1**, 73–95 (1974).